

Preoperative Prediction of Breast Cancer Histological Grade Using Intratumoral and Peritumoral Radiomics Features from T2WI and DWI MR Sequences

Yaxin Guo^{1,*}, Jun Liao^{1,*}, Shunian Li¹, Yiyan Shang², Yunxia Wang², Qingxia Wu³, Yaping Wu¹, Meiyun Wang¹, Fengshan Yan¹, Hongna Tan¹

¹Department of Radiology, People's Hospital of Zhengzhou University & Henan Provincial People's Hospital, Zhengzhou, People's Republic of China;

²Department of Radiology, People's Hospital of Henan University, Zhengzhou, People's Republic of China; ³Beijing United Imaging Research Institute of Intelligent Imaging & United Imaging Intelligence (Beijing) Co., Ltd, Beijing, People's Republic of China

*These authors contributed equally to this work

Correspondence: Hongna Tan; Fengshan Yan, Department of Radiology, People's Hospital of Zhengzhou University & Henan Provincial People's Hospital, Weiwu Road, Zhengzhou City, 450003, People's Republic of China, Tel +86-13526766042; +86-18637134815, Email natan2000@126.com; mounytan857@163.com

Background: Histological grade is an acknowledged prognostic factor for breast cancer, essential for determining clinical treatment strategies and prognosis assessment. Our study aims to establish intra- and peritumoral radiomics models using T2WI and DWI MR sequences for predicting the histological grade of breast cancer.

Methods: 700 breast cancer cases who had MRI scans before surgery were included. The intratumoral region (ITR) of interest was manually delineated, while the peritumoral region (PTR-3 mm) was automatically obtained by expanding the ITR by 3 mm. Radiomics features were extracted using the intra- and peritumoral images from T2WI and DWI sequences on breast MRI. Then, the key features with the strongest predictivity of histological grade were selected. Finally, 9 predictive radiomics models were established based on T2WI-ITR, T2WI-3mmPTR, DWI-ITR, DWI-3mmPTR, T2WI-ITR + 3mmPTR, DWI-ITR + 3mmPTR, (T2WI + DWI)-ITR, (T2WI + DWI)-3mmPTR and (T2WI + DWI)-ITR + 3mmPTR.

Results: The (T2WI + DWI)-ITR + 3mmPTR contained 13 DWI features which included a shape feature, a texture feature, and 11 filtered features, as well as 10 T2WI features, all of which were filtered features. Among the 9 models, the combined models showed better performance than the single models in both the training and test sets, especially for the (T2WI + DWI)-ITR + 3mmPTR radiomics model. The (T2WI + DWI)-ITR + 3mmPTR radiomics model achieved a sensitivity, specificity, accuracy, and AUC of 80.4%, 72.4%, 75.0%, and 0.860 in the training set, and 68.9%, 70.5%, 70.0%, and 0.781 in the test set. Decision curve analysis (DCA) showed that the (T2WI + DWI)-ITR + 3mmPTR model had the greatest net clinical benefit compared to the other models.

Conclusion: The intra- and peritumoral radiomics methodologies using T2WI and DWI MR sequences could be utilized to assess histological grade for breast cancer, particularly with the (T2WI + DWI)-ITR + 3mmPTR radiomics model demonstrating significant potential for clinical application.

Keywords: breast cancer, histological grade, MRI, T2WI, DWI, radiomics

Introduction

Breast cancer has become the most prevalent cancer among women.^{1,2} The outcome of breast cancer is affected by various factors, including molecular subtype, axillary lymph node (ALN) metastatic status, and histological grade. Among these factors, histological grade is a recognized prognostic indicator for breast cancer, which is critical for clinical therapeutic strategy and prognostic evaluation.³⁻⁶ Currently, the Nottingham grade system is widely used for histological grade of breast

cancer. This system is based on the assessment of the tubular formation, nuclear pleomorphism and mitotic count to assign a grade from I to III. Generally, a higher histological grade indicates a more malignant tumor and a worse prognosis. Clinically, pathology is still the most reliable method for evaluating histological grade. Conversely, this procedure is intrusive and may affect the accuracy of the results due to the heterogeneity of breast cancer.

Although mammography (MG), ultrasound (US), and MRI are common techniques used for diagnosing and evaluating breast cancer, these methods cannot provide accurate evaluation for tumor histological grade. Radiomics is a field that leverages the extraction and analysis of numerous quantitative features from medical images, such as CT scans, MRI, and PET images, to provide a more detailed characterization of tumors beyond what is possible with traditional visual assessment. This approach transforms images into high-dimensional, quantifiable data sets that can be analyzed to reveal patterns associated with disease diagnosis, prognosis, and treatment responses, enhancing personalized medicine and improving clinical outcomes.⁷⁻⁹ It has been demonstrated that radiomics possesses significant clinical applicability in diagnosing breast cancer, efficacy assessment, and prognosis evaluation.¹⁰⁻¹⁴ Because of high soft tissue resolution and capability for multi-sequence imaging, MRI is particularly valuable in breast cancer diagnosis and treatment. Especially for dynamic contrast-enhanced (DCE) imaging, it is of great significance in assessing tumor blood supply and detecting early-stage lesions. However, it is costly, time-consuming, and carries the risk of using the contrast agents. T2-weighted imaging (T2WI) has high accuracy and sensitivity for assessing normal anatomical structures and identifying various pathological changes, and diffusion-weighted imaging (DWI) can accurately show the early function of lesions without the need for contrast agents.

Breast cancer consists not only of tumor cells but also stromal cells, which play a crucial role in tumor growth, invasion, and metastasis. The peritumoral parenchyma often contains a series of pathophysiological information closely related to tumor development, which can indirectly affect the invasive and metastatic ability of tumor cells. Therefore, the peritumor parenchyma can also reflect the biological characteristics of cancer foci to a certain extent.

It is important to consider the stromal environment surrounding the tumor when studying breast cancer, as it reflects the tumor microenvironment and may contain valuable information about the aggressiveness of the cancer. Biologically, this region includes the reactive stroma, immune infiltration and vascular changes associated with the tumor, which may influence its behavior and progression.¹⁵⁻¹⁸ At present, there are still few studies published on using intra- and peritumoral radiomics features in predicting histological grade. The aim of our investigation is to establish the intra- and peritumoral radiomics models using T2WI and DWI for predicting the histological grade of breast cancer, in addition to providing a reference for individualized treatment and prognostic assessment.

Materials and Methods

Study Population

This retrospective study was conducted following the Declaration of Helsinki and was approved by the review board of Henan Provincial People's Hospital (NO. 2022-124), which waived the requirement for informed consent due to the study's retrospective nature. We declared that patient data remained confidential. About 730 subjects confirmed with invasive breast cancer were retrospectively enrolled from Jan 2017 to Dec 2020. Patients with definite histological grade results were included. Conversely, those with unavailable data, or who had a biopsy procedure, or chemoradiotherapy before MRI were excluded. Finally, 700 patients were enrolled (histological grade I:23; II:453; III:224). Histological grade I and II cases were combined because there were relatively few histological grade I cases. The dataset was allocated to a training set (n=560) as well as a test set (n=140) with an 8:2 proportion. The flowchart is presented in [Figure 1](#).

Clinicopathological Characteristics

Clinicopathological characteristics included patient age, menstrual condition, lesion size, location, histological grade, the expression of estrogen receptor (ER) (low: <10%, high: ≥10%), progesterone receptor (PR) (low: ≤20%, high: >20%), Ki-67 proliferation index (low: ≤20%, high: >20%) and human epidermal growth factor receptor2 (HER2).^{19,20}

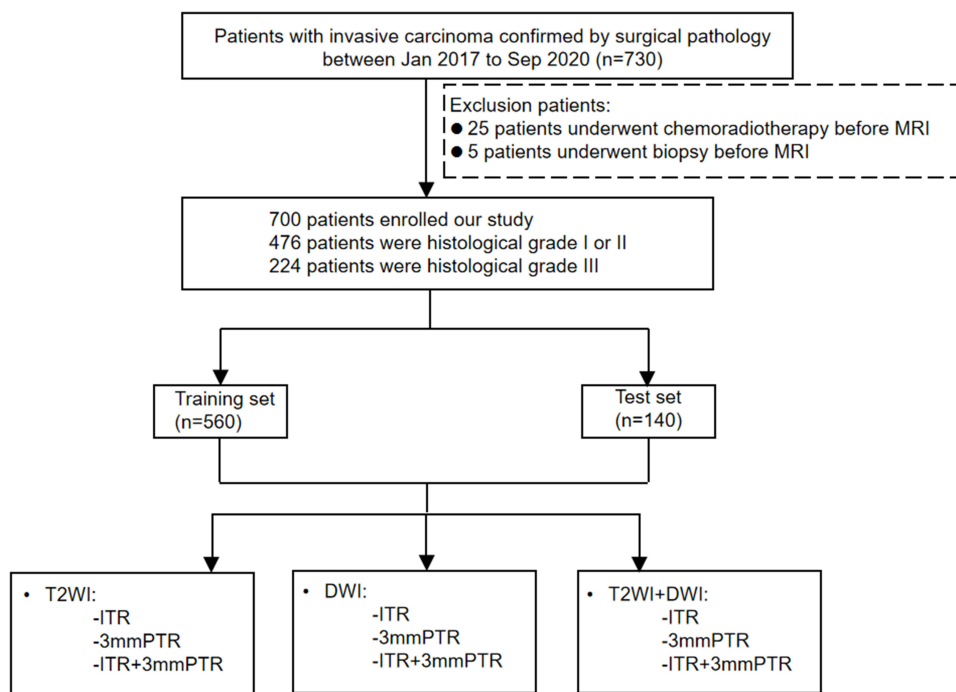


Figure 1 Workflow of Radiomics Analysis.

Abbreviations: DWI, diffusion-weighted imaging; T2WI, T2-weighted imaging; ITR, intratumoral region; PTR, peritumoral region.

Imaging Protocol and Image Segmentation

A 3.0-T MR scanner (GE Medical Systems, Milwaukee, WI) was conducted. Axial T2WI and DWI were obtained for each subject. The parameter details are provided in [Supplementary Information](#). Axial T2WI and DWI sequence images were archived in DICOM format. Using ITK-SNAP software (Version 3.8.0, <http://www.itk-snap.org>), a radiologist with over 6 years of expertise manually outlined the intratumoral region (ITR) layer-by-layer. While excluding regions of cystic necrosis and hemorrhage, the radiologist remained unaware of the patients' clinicopathological information. If there were multiple lesions on MRI, the largest lesion's region of interest (ROI) was selected. The delineated ITRs were then validated by a deputy chief physician with more than a decade of experience. The peritumoral region (PTR) was obtained by expanding the ITR outward by 3 mm through the use of the uRP platform (uAI research portal, <https://www.uai-ai.com/en/uai/scientific-research>)²¹ (Figure 2).

Feature Extraction and Selection

Radiomics features were computed with the original MRI scans and extracted through the uRP platform. Feature selection is used to select a subset of relevant features for use in model construction and the goal is to improve the model's performance by eliminating irrelevant or redundant data that could potentially lead to decreased accuracy and efficiency. The analysis of all extracted features was conducted through the following steps in this study. First, the radiomics features with the strongest predictivity of histological grade were selected using the Mann–Whitney *U*-test. Second, *Z* score normalization, a calculation with a mean of 0 and a standard deviation of 1, was used to reduce feature dimensionality differences. Then, features with high *p*-values were filtered out using the K-Best method (F value method, *K*=100). Finally, the most predictive radiomics features for histological grade were selected using the least absolute shrinkage and selection operator (LASSO) algorithm. Detailed information about the features can be found in the [Supplementary Information](#).

Model Establish and Evaluation

The radiomics features with the strongest predictivity of histological grade were selected from T2WI-ITR, T2WI-3mmPTR, DWI-ITR, DWI-3mmPTR, T2WI-ITR + 3mmPTR, DWI-ITR + 3mmPTR, (T2WI + DWI)-ITR, (T2WI + DWI)-3mmPTR and (T2WI + DWI)-ITR + 3mm PTR, respectively. Then classification models are used to predict the histological grade based

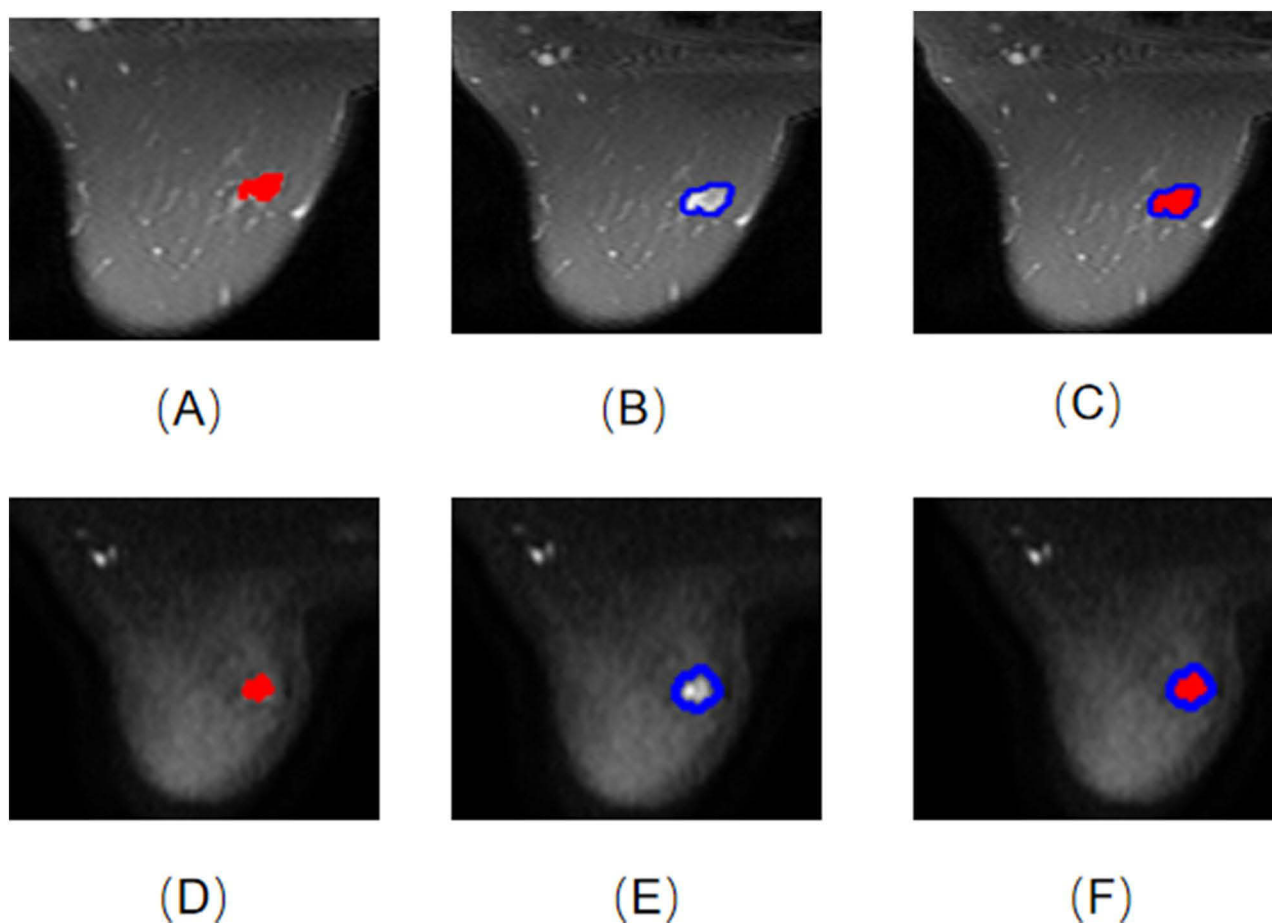


Figure 2 ROIs of 9 models. (A) T2WI-ITR; (B) T2WI-3mmPTR; (C) T2WI-ITR + 3mmPTR; (D) DWI-ITR; (E) DWI-3mmPTR; (F) DWI-ITR + 3mmPTR. **Abbreviation:** ROI, region of interest.

on these features and popular classification models in radiomics include Random Forests, Support Vector Machines (SVM) and so on. Additionally, a Gaussian process was utilized to transform these features into a probabilistic space, facilitating a more flexible and powerful modeling of the relationships between image features and their associated histological classes. In this study, the Gaussian process was utilized to develop 9 predictive models. The performance of these models was evaluated based on sensitivity, specificity, accuracy, and the area under the receiver operating characteristic (ROC) curve (AUC).

Statistical Analysis

Statistical analysis was conducted using SPSS software (V.25.0). For the continuous variables, Kolmogorov–Smirnov and Levene were used for normality and homogeneity of variance tests. Variables that follow a normal distribution were compared using an independent-sample *t*-test. For variables with a skewed distribution, the Mann–Whitney *U*-test was utilized for group comparisons. Categorical variables were compared using the chi-square test. $P < 0.05$ was considered statistically significant.

Results

Clinical Findings

This study included 700 female breast cancer patients (histological grade I:23; II:453; III:224). There were no significant differences in the clinicopathological characteristics between the training and test sets (all $p > 0.05$) (Table 1). There were significant differences in terms of tumor size, HER2 status, ER status, PR status, and Ki-67 proliferation index between histological grade I + II and III patients (all $p < 0.05$), but there were no significant differences in the other characteristics ($p > 0.05$) (Table 2).

Table 1 Comparison of Clinicopathological Characteristics Between Training Set and Test Set

Characteristics	Training Set (n=560)	Test Set (n=140)	P
Age (Year, $\bar{x} \pm s$)	48.96 \pm 10.41	48.67 \pm 9.56	0.251 ^a
Menstrual status (%)			
Premenopausal	254(45.4)	51(36.4)	0.057 ^b
Postmenopausal	306(54.6)	89(63.6)	
Location of disease (%)			
Left breast	269(48.0)	72(51.4)	0.473 ^b
Right breast	291(52.0)	68(48.6)	
Tumor size [M (Q1, Q3)]mm	20(15,29)	22(16,27)	0.649 ^c
HER2 status (%)			
Negative	415(74.1)	101(72.1)	0.637 ^b
Positive	145(25.9)	39(27.9)	
ER status (%)			
<10%	148(26.4)	41(29.3)	0.496 ^b
\geq 10%	412(73.6)	99(70.7)	
PR status (%)			
\leq 20%	280(50.0)	75(53.6)	0.450 ^b
>20%	280(50.0)	65(46.4)	
Ki-67 (%)			
\leq 20%	216(38.6)	58(41.4)	0.536 ^b
>20%	344(61.4)	82(58.6)	

Notes: ^aindependent-sample t-test; ^bchi-square test; ^cMann-Whitney U-test.

Table 2 Comparison of Clinicopathological Characteristics Between Histological Grade I + II and Grade III Groups

Characteristics	Training Set (n=560)		P	Test Set (n=140)		P
	Grade I+II (n=381)	Grade III (n=179)		Grade I+II (n=95)	Grade III (n=45)	
Age (Year, $\bar{x} \pm s$)	48.88 \pm 10.18	49.13 \pm 10.91	0.168 ^a	49.12 \pm 8.85	47.73 \pm 10.95	0.075 ^a
Menstrual status (%)						
Premenopausal	214 (56.17)	92 (51.40)	0.290 ^b	61(64.21)	28 (62.22)	0.819 ^b
Postmenopausal	167 (43.83)	87 (48.60)		34 (35.79)	17 (37.78)	
Location of disease (%)						
Left breast	183 (48.03)	86 (48.04)	0.998 ^b	48 (50.52)	24 (53.33)	0.756 ^b
Right breast	198 (51.97)	93 (51.96)		47 (49.47)	21 (46.67)	
Tumor size [M (Q1, Q3)]mm	20 (15,26)	25 (19,34)	<0.001^c	20 (14,26)	23 (19,28)	<0.001^c
HER2 status (%)						
Positive	87 (22.83)	58 (32.40)	0.016^b	20 (21.05)	19 (42.22)	0.009^b
Negative	294 (77.17)	121 (67.60)		75 (78.95)	26 (57.78)	
ER status (%)						
<10%	57 (14.96)	91 (50.84)	<0.001^b	16 (16.84)	25 (55.56)	<0.001^b
\geq 10%	324 (85.04)	88 (49.16)		79 (83.16)	20 (44.44)	
PR status (%)						
\leq 20%	150 (39.37)	130 (72.63)	<0.001^b	40 (42.11)	35 (77.78)	<0.001^b
>20%	231 (60.63)	49 (27.37)		55 (57.89)	10 (22.22)	
Ki-67 (%)						
\leq 20%	197 (51.71)	19 (10.61)	<0.001^b	52 (54.74)	6 (13.33)	<0.001^b
>20%	184 (48.29)	160 (89.39)		43 (45.26)	39 (86.67)	

Notes: ^aindependent-sample t-test; ^bchi-square test; ^cMann-Whitney U-test. The bold values presented indicate statistically significant p-values.

Abbreviations: HER2, human epidermal growth factor receptor 2; ER, estrogen receptor; PR, progesterone receptor.

Feature Extraction and Selection

Using the LASSO regression method, the optimal features were selected, resulting in the selection of 7, 2, 21, 8, 14, 17, 7, 8, and 23 radiomics features from T2WI-ITR, T2WI-3mmPTR, DWI-ITR, DWI-3mmPTR, T2WI-ITR + 3mmPTR, DWI-ITR + 3mmPTR, (T2WI + DWI)-ITR, (T2WI + DWI)-3mmPTR and (T2WI + DWI)-ITR + 3mmPTR images, respectively. The (T2WI + DWI)-ITR + 3mmPTR contained 13 DWI features which included a shape feature, a texture feature, and 11 filtered features, as well as 10 T2WI features, all of which were filtered features. Detailed information about the features can be found in the [Supplementary Information](#).

Construction and Validation of Models

Table 3 presents the detailed predictive performance of radiomics models based on T2WI and DWI. The AUCs of the 9 models, constructed using radiomics features from T2WI-ITR, T2WI-3mmPTR, DWI-ITR, DWI-3mmPTR, T2WI-ITR + 3mmPTR, DWI-ITR + 3mmPTR, (T2WI + DWI)-ITR, (T2WI + DWI)-3mmPTR, and (T2WI + DWI)-ITR + 3mmPTR, were 0.733, 0.707, 0.750, 0.724, 0.790, 0.833, 0.791, 0.765, and 0.860 for the training set, and 0.739, 0.705, 0.723, 0.718, 0.758, 0.759, 0.753, 0.746, and 0.781 for the test set, respectively (Figure 3). The (T2WI + DWI)-ITR + 3mmPTR radiomics model achieved a sensitivity, specificity, accuracy, and AUC of 80.4%, 72.4%, 75.0%, and 0.860 in the training set, and 68.9%, 70.5%, 70.0%, and 0.781 in the test set (Figure 4). Decision curve analysis (DCA) showed that the (T2WI + DWI)-ITR + 3mmPTR radiomics model provided the greatest clinical net benefit over a threshold probability range of 0.02 to 0.88 (Figure 5).

Discussion

In this study, intra- and peritumoral radiomics models were developed to accurately predict the histological grade of breast cancer patients preoperatively. Especially, the (T2WI + DWI)-ITR + 3mmPTR radiomics model was clinically useful to help therapeutic strategy optimization.

The possible reasons for the differences between histological grade I + II and III patients are as follows. First, tumor size, which is a key indicator to assess the degree of tumor growth and invasion, is essential for the selection of surgical modality and prognostic assessment. Previous studies have demonstrated that larger tumors tend to have higher histological grades, which may be attributed to their faster growth rate and higher aggressiveness.²² Consistent with these findings, our study revealed that patients with histological grade I + II had smaller lesion diameters compared to those with histological grade III. Second, HER2, ER, and PR status are key factors in determining endocrine therapy and targeted therapy, helping physicians determine the appropriate treatment options. HER2, a receptor exhibiting tyrosine kinase activity, is vital for tumor cell growth and proliferation, and HER2-positive patients may benefit from targeted therapy. Our study found that cases with histological grade III tended to have a higher HER2 expression status than patients with histological grade II (training set: 32.40% vs 22.83%; test set: 42.22% vs 21.05%). These results agree with those reported by Takahashi et al.²³ ER and PR are hormone receptors in tumor cells. Our study revealed that patients

Table 3 Predictive Performances of 9 Radiomics Models

Models	Training Set (n=560)				Test Set (n=140)			
	AUC (95% CI)	Sensitivity	Specificity	Accuracy	AUC (95% CI)	Sensitivity	Specificity	Accuracy
T2WI- ITR	0.733 (0.690–0.775)	60.3%	68.8%	66.1%	0.739 (0.656–0.822)	73.3%	58.9%	63.6%
T2WI- PTR	0.707 (0.664–0.751)	65.4%	63.5%	64.1%	0.705 (0.615–0.795)	62.2%	60.0%	60.7%
T2WI+ITR + PTR	0.790 (0.753–0.828)	77.7%	62.2%	67.1%	0.758 (0.678–0.839)	71.1%	62.1%	65.0%
DWI- ITR	0.750 (0.709–0.792)	72.6%	63.3%	66.2%	0.723 (0.637–0.809)	71.1%	62.1%	65.0%
DWI-PTR	0.724 (0.682–0.767)	71.5%	61.4%	64.6%	0.718 (0.633–0.803)	77.8%	60.0%	65.7%
DWI+ITR + PTR	0.833 (0.799–0.867)	76.5%	74.3%	75.0%	0.759 (0.679–0.839)	60.0%	70.5%	67.1%
(T2WI + DWI)-ITR	0.791 (0.754–0.829)	70.9%	71.1%	71.1%	0.753 (0.674–0.832)	64.4%	67.4%	66.4%
(T2WI + DWI)-PTR	0.765 (0.726–0.804)	68.7%	66.7%	67.3%	0.746 (0.666–0.826)	73.3%	65.3%	67.9%
(T2WI + DWI)-ITR + PTR	0.860 (0.829–0.892)	80.4%	72.4%	75.0%	0.781 (0.702–0.859)	68.9%	70.5%	70.0%

Abbreviations: AUC, area under the receiver operating characteristic curve; CI, confidence interval.

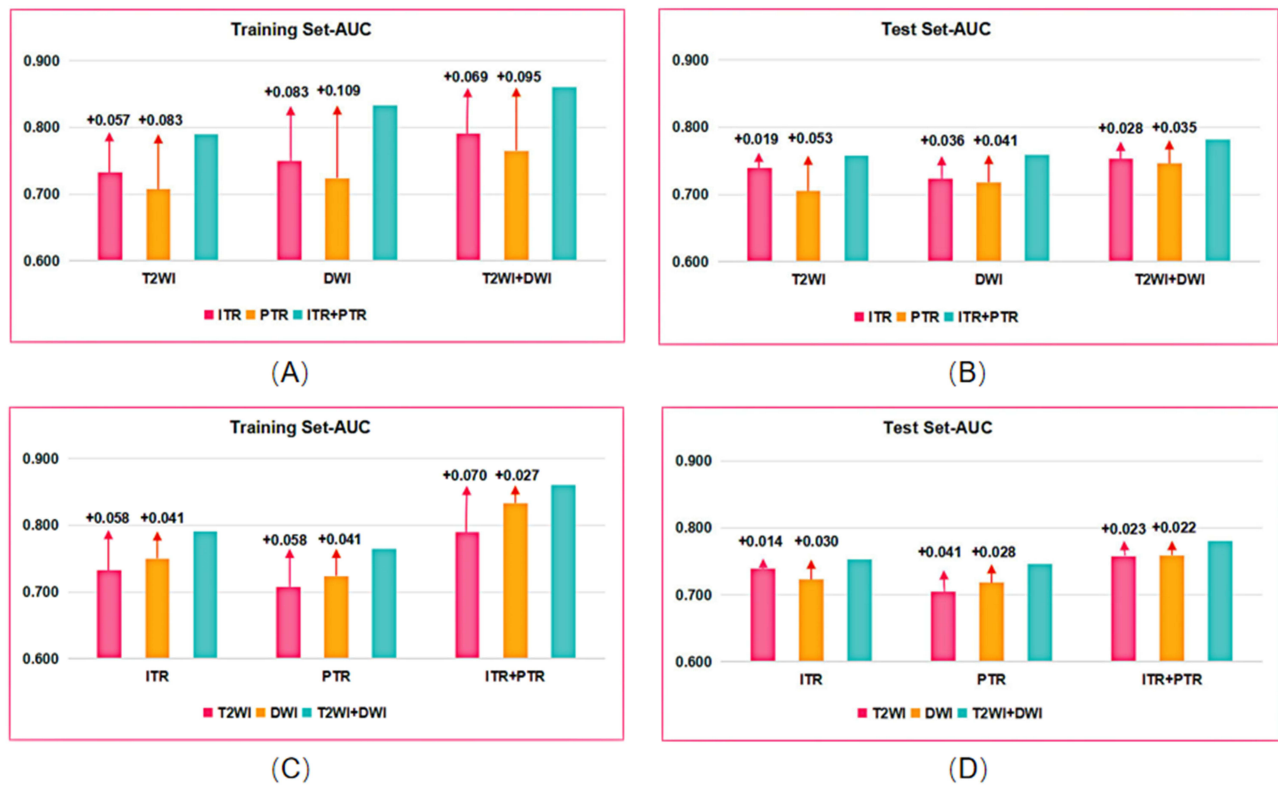


Figure 3 Comparison of AUC between the combined models and the single models in the training and test sets. **(A and B)** Comparison of AUC between the combined sequence-models and the single sequence-models in the training **(A)** and test sets **(B)**. **(C and D)** Comparison of AUC between the ITR+PTR-models and the single ITR or PTR-model in the training **(C)** and test sets **(D)**.

Abbreviation: AUC, area under the receiver operating characteristic curve.

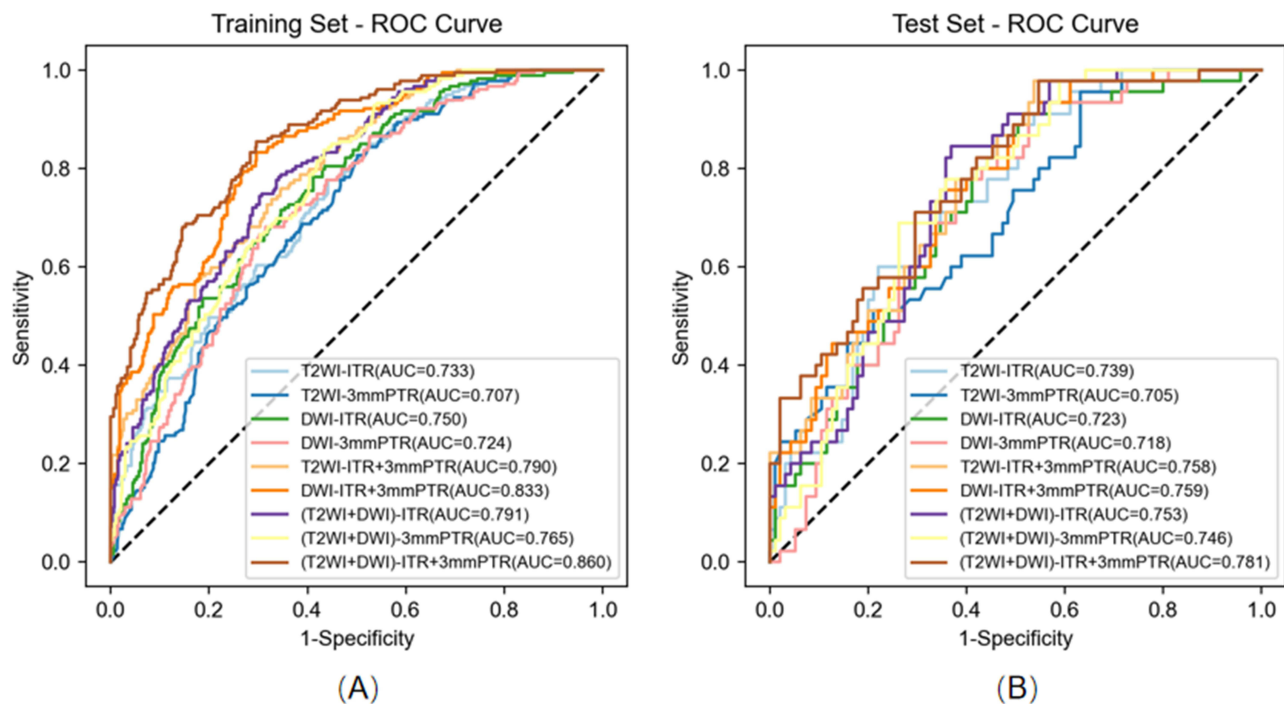


Figure 4 Receiver operator characteristic (ROC) curves of nine models. **(A)** Nine models of ROC curves in the training set. **(B)** Nine models of ROC curves in the test set.

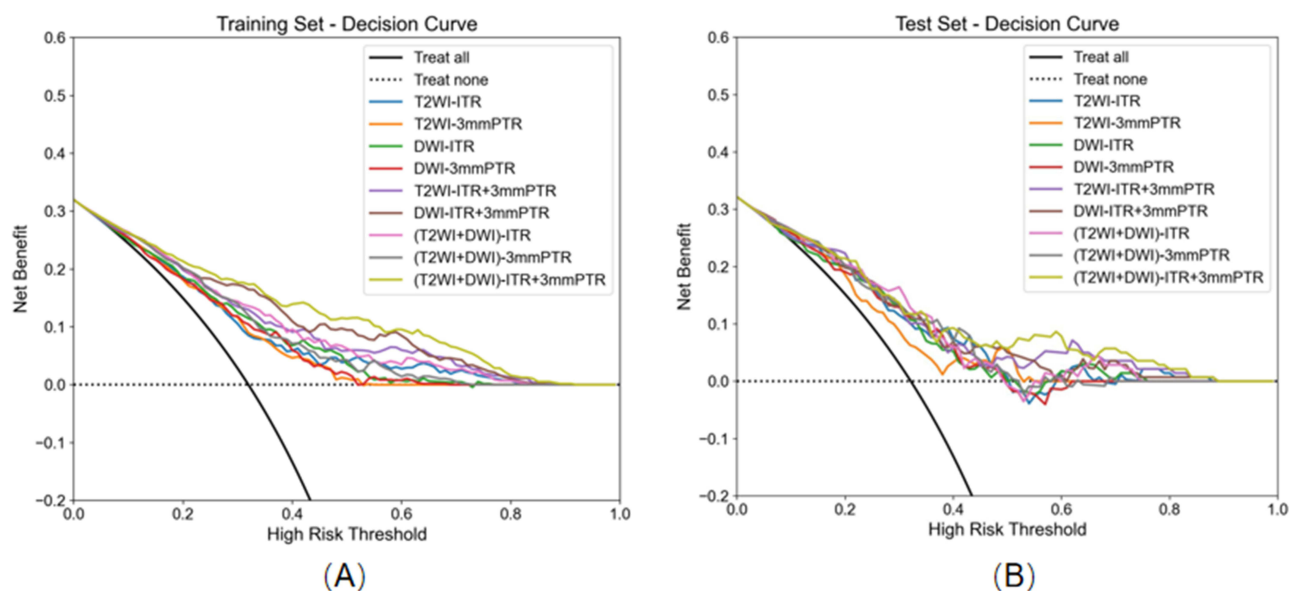


Figure 5 Decision curve analysis (DCA) of nine models. **(A)** Nine models of DCA in the training set. **(B)** Nine models of DCA in the test set.

with ER $\geq 10\%$ and PR $> 20\%$ had a higher proportion of histological grade I + II compared to grade III (training set: ER: 85.04% vs 49.16%, PR: 60.63% vs 27.37%; test set: ER: 83.16% vs 44.44%, PR: 57.89% vs 22.22%). These results correspond to the conclusions of Takahashi et al,²³ suggesting that higher levels of ER and PR correlate with lower histological grade. Finally, Ki-67 is a measure of cellular proliferation and correlates with the degree of tumor cellular activation. Liang et al argued that patients with higher expression of Ki-67 tend to have higher histological grades.²⁴ Consistent with this, our study found that the percentage of patients with Ki-67 $> 20\%$ in histological grade III surpassed that in grade I + II (training set: 89.39% vs 48.29%, test set: 86.67% vs 45.26%). Therefore, taking into account the clinicopathological differences between histological grade I + II and III, it is possible to explore how to refer to these clinicopathological indicators in the future, to determine the prioritization and combination of treatments to improve treatment efficacy and patient survival.

Radiomics methods have been shown to preoperatively predict histological grade in breast tumors.^{25–27} However, further study on the value of T2WI and DWI radiomics on breast MRI for preoperatively predicting histological grade is still needed. In our study, we found that the AUCs for T2WI combined with DWI sequences were improved compared to that of the single T2WI or DWI sequence, regardless of whether the model was intratumoral, peritumoral, or intratumoral combined with peritumoral. Rong et al conducted a previous study that indicated mammography-based radiomics nomograms achieved AUCs of 0.750 in preoperatively predicting the histological grade of invasive ductal carcinoma.²⁵ The predictive performance of our single-sequence intratumoral model was slightly lower compared to the previously mentioned study. However, the performances of our intratumoral combined peritumoral or multi-sequence combination models were superior. Additionally, in another study, our T2WI + DWI-ITR models showed higher AUCs compared to those reported by Fan et al (training set: 0.788; test set: 0.744), who used radiomics features based on DCE-MRI and T2WI to predict breast cancer histological grades,²⁶ and this may be related to the different choice of the study sequences, and the radiomics features of DWI used in our study may reflect tumor heterogeneity better than the features of DCE-MRI. Compared to Wang's study which used radiomics features based on DCE-MRI to predict the histological grade of breast cancers,²⁷ we found that the AUCs in our study were higher than those of Wang et al in the test set (AUC:0.720).

The peritumor parenchyma can further reflect the biological characteristics of cancer foci. Previous studies have demonstrated the strong predictive effect of intratumoral combined with peritumoral radiomics features in breast cancer diagnosis, lymph node metastasis (LNM), and neoadjuvant chemotherapy response.^{28–30} Our research revealed that the peritumoral radiomics features in both T2WI, DWI, and T2WI + DWI sequences showed promising predictive efficacy for the histological grade in breast cancer, with AUCs of ≥ 0.700 . Furthermore, the AUC of the intratumoral + peritumoral models

outperformed that of the single intra- or peritumoral models (T2WI:0.758>0.739, 0.705; DWI:0.759>0.723, 0.718; T2WI + DWI:0.781>0.753, 0.746). Although the ideal size of the peritumoral region remains uncertain, it has been observed that the efficacy of the radiomics model may decline as the peritumoral radius increases within a certain range.^{30,31} In one study by Mao et al³⁰ on the value of predicting the outcome of NAC for breast cancer using contrast-enhanced spectral mammography (CESM) radiomics features, they explored the predictive efficacy of different peritumoral radii (5mmPTR, 10mmPTR) and the combination of intra- and peritumoral radiomics features. They confirmed that the prediction efficacy of the ITR combined with 5mmPTR radiomics model (AUC: training set:0.870; test set:0.850) was higher than that of the ITR combined with 10 mm PTR radiomics model (AUC: training set:0.810; test set:0.840). In another research, Park et al³¹ demonstrated that the prediction capability of the ITR combined with 1mmPTR radiomics model exceeded that of the ITR combined with 3mmPTR radiomics model for predicting neoadjuvant chemotherapy (NAC) pathological complete response, regardless of the early stage of the enhanced scan (AUC:0.940>0.900), the late stage of the enhanced scan (AUC:0.890>0.720), or the T2WI sequence (AUC:0.920>0.870).

The AUCs of the test set of the 9 models based on the radiomics features of T2WI-ITR, T2WI-3mmPTR, DWI-ITR, DWI-3mmPTR, T2WI-ITR + 3mmPTR, DWI-ITR + 3mmPTR, (T2WI + DWI)-ITR, (T2WI + DWI)-3mmPTR and (T2WI + DWI)-ITR + 3mmPTR were 0.739, 0.705, 0.723, 0.718, 0.758, 0.759, 0.753, 0.746, 0.781, respectively. Taking into account the multiple MRI sequences and the peritumoral microenvironment to conduct radiomics analysis from multiple angles and dimensions, the 9 radiomics prediction models in our study can help physicians more accurately assess the biology and aggressiveness of breast cancer in a clinical setting, thereby guiding preoperative decision-making. For example, local treatments such as breast-conserving surgery or local excision may be considered for patients with a low-grade tumor, while a wider range of treatment options such as surgical resection or chemotherapy may be considered for patients with a high-grade tumor.^{32,33}

Our study had several limitations. First, radiologists manually outline the ROI for breast cancer lesions, a procedure that is time-consuming, subjective, error-prone, and not scalable with increasing data volumes. Therefore, an automated, standardized, repeatable, and validated segmentation method would be more practical for future use. Second, our study was a single-center retrospective investigation, and there was a lack of external validation, which needs to be further improved. Third, fewer histological grade I patients were classified as grade II, which may bias the results. Increasing the sample size, using multicenter data, or improving classification methods could improve the results. Finally, the peritumoral region was defined by expanding the tumor outward by 3 mm. However, further research is needed to determine whether this extension is optimal. Future work should refine and validate this extension to determine its effectiveness.

Conclusion

In conclusion, our study indicates that intratumoral and peritumoral radiomics methods based on T2WI and DWI MR sequences were helpful in predicting breast cancer histological grade, especially for the intratumoral + peritumoral radiomics method based on combined T2WI + DWI sequences showing the highest predictive performance. It is expected to be a dependable clinical tool for histological grade prediction, which potentially enhances clinicians' ability to make personalized treatment decisions.

Data Sharing Statement

The dataset used in this study is available from the corresponding author upon reasonable request.

Ethical Approval

This study was approved by the Research Ethics Committee of the Henan Provincial People's Hospital (No. 2022-124).

Informed Consent

Informed consents were waived due to the study's retrospective nature. We declared that patient data remained confidential.

Acknowledgments

The authors wish to thank all the study participants, research staff, and students who participated in this work.

Funding

This study was supported by the Henan Provincial Medical Science and Technology Research Program (LHGJ20220055).

Disclosure

Professor Meiyun Wang reports a patent A magnetic resonance detector licensed to Meiyun Wang, a patent Tumor nano-diagnostic and therapeutic agent for combined therapy guided by multi-responsive dual-modal imaging and preparation method thereof licensed to Meiyun Wang. The authors declare that they have no other conflicts of interest.

References

1. Siegel RL, Giaquinto AN, Jemal A. Cancer statistics, 2024. *CA Cancer J Clin*. 2024;74(1):12–49. doi:10.3322/caac.21820
2. Loibl S, Poortmans P, Morrow M, Denkert C, Curigliano G. Breast cancer. *Lancet*. 2021;397(10286):1750–1769. doi:10.1016/S0140-6736(20)32381-3
3. Rakha EA, El-Sayed ME, Lee AH, et al. Prognostic significance of Nottingham histologic grade in invasive breast carcinoma. *J Clin Oncol*. 2008;26(19):3153–3158. doi:10.1200/JCO.2007.15.5986
4. Gradishar WJ, Moran MS, Abraham J, et al. NCCN Guidelines® Insights: breast Cancer, Version 4.2023. *J Natl Compr Canc Netw*. 2023;21(6):594–608. doi:10.6004/jnccn.2023.0031
5. Abubakar M, Chang-Claude J, Ali HR, et al. Etiology of hormone receptor positive breast cancer differs by levels of histologic grade and proliferation. *Int J Cancer*. 2018;143(4):746–757. doi:10.1002/ijc.31352
6. Zhang Y, Zhou Y, Mao F, Yao R, Sun Q. Ki-67 index, progesterone receptor expression, histologic grade and tumor size in predicting breast cancer recurrence risk: a consecutive cohort study. *Cancer Commun*. 2020;40(4):181–193. doi:10.1002/cac2.12024
7. Guiot J, Vaidyanathan A, Deprez L, et al. A review in radiomics: making personalized medicine a reality via routine imaging. *Med Res Rev*. 2022;42(1):426–440. doi:10.1002/med.21846
8. Mayerhoefer ME, Materka A, Langs G, et al. Introduction to Radiomics. *J Nucl Med*. 2020;61(4):488–495. doi:10.2967/jnumed.118.222893
9. Neri E, Del Re M, Paia F, et al. Radiomics and liquid biopsy in oncology: the holons of systems medicine. *Insights Imaging*. 2018;9(6):915–924. doi:10.1007/s13244-018-0657-7
10. Valdora F, Houssami N, Rossi F, Calabrese M, Tagliafico AS. Rapid review: radiomics and breast cancer. *Breast Cancer Res Treat*. 2018;169(2):217–229. doi:10.1007/s10549-018-4675-4
11. Liu Z, Wang S, Dong D, et al. The Applications of Radiomics in Precision Diagnosis and Treatment of Oncology: opportunities and Challenges. *Theranostics*. 2019;9(5):1303–1322. doi:10.7150/thno.30309
12. Guo Y, Xie X, Tang W, et al. Noninvasive identification of HER2-low-positive status by MRI-based deep learning radiomics predicts the disease-free survival of patients with breast cancer. *Eur Radiol*. 2024;34(2):899–913. doi:10.1007/s00330-023-09990-6
13. Chen Y, Li J, Zhang J, Yu Z, Jiang H. Radiomic Nomogram for Predicting Axillary Lymph Node Metastasis in Patients with Breast Cancer. *Acad Radiol*. 2024;31(3):788–799. doi:10.1016/j.acra.2023.10.026
14. Du Y, Cai M, Zha H, et al. Ultrasound radiomics-based nomogram to predict lymphovascular invasion in invasive breast cancer: a multicenter, retrospective study. *Eur Radiol*. 2024;34(1):136–148. doi:10.1007/s00330-023-09995-1
15. Ma Y, Guan Z, Liang H, Cao H. Predicting the WHO/ISUP Grade of Clear Cell Renal Cell Carcinoma Through CT-Based Tumoral and Peritumoral Radiomics. *Front Oncol*. 2022;12:831112. doi:10.3389/fonc.2022.831112
16. Liu Z, Mi M, Li X, Zheng X, Wu G, Zhang L. A lncRNA prognostic signature associated with immune infiltration and tumour mutation burden in breast cancer. *J Cell Mol Med*. 2020;24(21):12444–12456. doi:10.1111/jcmm.15762
17. Cheon H, Kim HJ, Kim TH, et al. Invasive Breast Cancer: prognostic Value of Peritumoral Edema Identified at Preoperative MR Imaging. *Radiology*. 2018;287(1):68–75. doi:10.1148/radiol.2017171157
18. Kwon BR, Shin SU, Kim SY, et al. Microcalcifications and Peritumoral Edema Predict Survival Outcome in Luminal Breast Cancer Treated with Neoadjuvant Chemotherapy. *Radiology*. 2022;304(2):310–319. doi:10.1148/radiol.211509
19. Prat A, Cheang MC, Martín M, et al. Prognostic significance of progesterone receptor-positive tumor cells within immunohistochemically defined luminal A breast cancer. *J Clin Oncol*. 2013;31(2):203–209. doi:10.1200/JCO.2012.43.4134
20. Allison KH, Hammond M, Dowsett M, et al. Estrogen and Progesterone Receptor Testing in Breast Cancer: ASCO/CAP Guideline Update. *J Clin Oncol*. 2020;38(12):1346–1366. doi:10.1200/JCO.19.02309
21. Wu J, Xia Y, Wang X, et al. uRP: an integrated research platform for one-stop analysis of medical images. *Front Radiol*. 2023;3:1153784. doi:10.3389/fradi.2023.1153784
22. Hariharan N, Rao TS, Naidu CK, et al. The Impact of Stage and Molecular Subtypes on Survival Outcomes in Young Women with Breast Cancer. *J Adolesc Young Adult Oncol*. 2019;8(5):628–634. doi:10.1089/jayao.2019.0023
23. Takahashi H, Oshi M, Asaoka M, Yan L, Endo I, Takabe K. Molecular Biological Features of Nottingham Histological Grade 3 Breast Cancers. *Ann Surg Oncol*. 2020;27(11):4475–4485. doi:10.1245/s10434-020-08608-1
24. Liang Q, Ma D, Gao RF, Yu KD. Effect of Ki-67 Expression Levels and Histological Grade on Breast Cancer Early Relapse in Patients with Different Immunohistochemical-based Subtypes. *Sci Rep*. 2020;10(1):7648. doi:10.1038/s41598-020-64523-1

25. Rong XC, Kang YH, Shi GF, et al. The use of mammography-based radiomics nomograms for the preoperative prediction of the histological grade of invasive ductal carcinoma. *J Cancer Res Clin Oncol*. 2023;149(13):11635–11645. doi:10.1007/s00432-023-05001-9
26. Fan M, Yuan W, Zhao W, et al. Joint Prediction of Breast Cancer Histological Grade and Ki-67 Expression Level Based on DCE-MRI and DWI Radiomics. *IEEE J Biomed Health Inform*. 2020;24(6):1632–1642. doi:10.1109/JBHI.2019.2956351
27. Wang S, Wei Y, Li Z, Xu J, Zhou Y. Development and Validation of an MRI Radiomics-Based Signature to Predict Histological Grade in Patients with Invasive Breast Cancer. *Breast Cancer*. 2022;14:335–342. doi:10.2147/BCTT.S380651
28. Huang Z, Mo S, Wu H, et al. Optimizing breast cancer diagnosis with photoacoustic imaging: an analysis of intratumoral and peritumoral radiomics. *Photoacoustics*. 2024;38:100606. doi:10.1016/j.pacs.2024.100606
29. Zhang W, Wang S, Wang Y, et al. Ultrasound-based radiomics nomogram for predicting axillary lymph node metastasis in early-stage breast cancer. *Radiol Med*. 2024;129(2):211–221. doi:10.1007/s11547-024-01768-0
30. Mao N, Shi Y, Lian C, et al. Intratumoral and peritumoral radiomics for preoperative prediction of neoadjuvant chemotherapy effect in breast cancer based on contrast-enhanced spectral mammography. *Eur Radiol*. 2022;32(5):3207–3219. doi:10.1007/s00330-021-08414-7
31. Park J, Kim MJ, Yoon JH, et al. Machine Learning Predicts Pathologic Complete Response to Neoadjuvant Chemotherapy for ER+HER2- Breast Cancer: integrating Tumoral and Peritumoral MRI Radiomic Features. *Diagnostics*. 2023;13(19):3031. doi:10.3390/diagnostics13193031
32. Chua BH, Link EK, Kunkler IH, et al. Radiation doses and fractionation schedules in non-low-risk ductal carcinoma in situ in the breast (BIG 3-07/TROG 07.01): a randomised, factorial, multicentre, open-label, Phase 3 study. *Lancet*. 2022;400(10350):431–440. doi:10.1016/S0140-6736(22)01246-6
33. Stenmark Tullberg A, Sjöström M, Tran L, et al. Combining histological grade, TILs, and the PD-1/PD-L1 pathway to identify immunogenic tumors and de-escalate radiotherapy in early breast cancer: a secondary analysis of a randomized clinical trial. *J Immunother Cancer*. 2023;11(5):e006618. doi:10.1136/jitc-2022-006618

Breast Cancer: Targets and Therapy

Dovepress

Publish your work in this journal

Breast Cancer - Targets and Therapy is an international, peer-reviewed open access journal focusing on breast cancer research, identification of therapeutic targets and the optimal use of preventative and integrated treatment interventions to achieve improved outcomes, enhanced survival and quality of life for the cancer patient. The manuscript management system is completely online and includes a very quick and fair peer-review system, which is all easy to use. Visit <http://www.dovepress.com/testimonials.php> to read real quotes from published authors.

Submit your manuscript here: <https://www.dovepress.com/breast-cancer—targets-and-therapy-journal>